DOI: 10.1002/ejic.200900598

Characteristic Structures and Photophysical Properties of Nine-Coordinate Europium(III) Complexes with Tandem-Connected Tridentate Phosphane Oxide Ligands

Kohei Miyata,[a] Yasuchika Hasegawa,*[a] Yusuke Kuramochi,[a] Tetsuya Nakagawa,[a] Toshiaki Yokoo,[b] and Tsuyoshi Kawai*[a]

Keywords: Luminescence / Tridentate ligands / Lanthanides / Ligand effects

Structures and photophysical properties of *f*-block metal complexes with tandem-connected tridentate phosphane oxide ligands, {bis[*o*-(diphenylphosphoryl)phenyl]phenylphosphane oxide}tris(hexafluoroacetylacetonato)europium(III) [Eu(hfa)$_3$(DPPPO)], {bis[*o*-(diphenylphosphoryl)pyridyl]-phenylphosphane oxide}tris(hexafluoroacetylacetonato)europium(III) [Eu(hfa)$_3$(DPPYPO)] and {bis[*o*-(diphenylphosphoryl)benzothienyl]phenylphosphane oxide}tris(hexafluoroacetylacetonato)europium(III) [Eu(hfa)$_3$(DPBTPO)], are reported. The coordination geometries of Eu(hfa)$_3$(DPPPO) and Eu(hfa)$_3$(DPBTPO) provide characteristic distorted, capped square antiprism structures with nine-coordinate oxygen atoms. The emission properties related to the electric transition are characterized by the emission spectra, the emission quantum yields, the emission lifetimes, and the radiative and non-radiative rate constants. Eu^{III} complexes with tridentate phosphane oxide ligands offer relatively high emission quantum yields (> 60 % in [D$_6$]acetone) due to their low-symmetric and low-frequency vibrational structures. The electric dipole transition intensities in the emission spectra depend on the chemical structures of tridentate phosphane oxides. The characteristic photophysical properties of polyhedral *f*-block metal complexes, nine-coordinate Eu^{III} complexes with tridentate phosphane oxide, are demonstrated for the first time.

Introduction

Lanthanide(III) complexes are regarded for use as luminescent materials for EL devices,[1] lasers[2] and luminescent bio-sensing applications.[3] The luminescence properties of lanthanide complexes such as Eu^{III}, Tb^{III}, Sm^{III}, Yb^{III} and Nd^{III} complexes are mainly derived from the electric transitions in *4f* orbitals. Generally, *4f* orbitals of lanthanide are shielded from direct perturbations by outer filled *5s* and *5p* shells.[4,5] The electric dipole transitions from the *4f* inner shell of lanthanide ions are intrinsically forbidden because of their odd parity. However, they can be partially allowed upon mixing *4f* and *5d* states through the ligand field effects. The partially allowed transitions and electrically shielded nature of the excited states promote long emission lifetimes and characteristic sharp emission bands. A large number of studies on the characteristic luminescence properties of lanthanide complexes have been reported.[6]

Radiative rate constants of the lanthanide complexes depend greatly on the geometrical symmetry of the coordination structure. Richardson and Reid have estimated the transition intensity parameters of lanthanide complexes from the ligand field.[7] Binnemans has proposed to evaluate the transition intensity by using Judd–Ofelt analysis.[8] Since these studies, it has been widely accepted that the radiative transition probability between *4f* orbitals is enhanced by reducing the coordination structure's geometrical symmetry.[9,10]

The emission properties of lanthanide complexes also depend on the vibronic properties, which dominate the kinetics of the non-radiative transition processes. According to the energy gap theory, the non-radiative transition processes are promoted by the presence of ligands and solvents with high-frequency vibrational modes.[11] In earlier studies, we have reported on the suppression of radiationless quenching in Nd^{III} systems in organic media by introducing diketonato ligands having C–F bonds with low-vibrational frequency (LVF) such as hexafluoroacetylacetonato: hfa.[12] The LVF ligands having C–F bonds instead of C–H bonds

[a] Graduate School of Materials Science, Nara Institute of Science and Technology,
8916-5, Takayama, Ikoma, Nara 630-0192, Japan
Fax: +81-743-72-6171
E-mail: hasegawa@ms.naist.jp
[b] Science & Technology Research Center, Mitsubishi Chemical Corporation,
1000 Kamoshida, Aoba, Yokohama 227-8502, Japan
Supporting information for this article is available on the WWW under http://dx.doi.org/10.1002/ejic.200900598.

effectively suppress the radiationless transition in the lanthanide complexes. Recently, the effect on the Ln–X vibrations have also been reported.[13]

In order to prepare intensely luminescent lanthanide complexes, a large radiative rate constant is necessary based on reducing the geometrical symmetry and small non-radiative rate constant by introducing LVF organic ligands. Previously, we have reported on Eu^{III} complexes with LVF ligands, hfa and triphenylphosphane oxide: TPPO [$Eu(hfa)_3(TPPO)_2$], for which the chemical structure is shown in Figure 1 (a).[14] The coordination structure composed of the LVF phosphane oxide (P=O: 1125 cm^{-1}) and hfa provides the Eu^{III} complex with a high emission quantum yield and a relatively small non-radiative rate constant. The coordination geometry of $Eu(hfa)_3(TPPO)_2$ is categorized as a distorted Square AntiPrism (8-SAP). The characteristic 8-SAP structure is composed of three hfa and two TPPO ligands, which leads to a reduction of the geometrical symmetry of the Eu^{III} complex and consequently $Eu(hfa)_3(TPPO)_2$ shows a relatively large radiative rate constant. We have also reported a Eu^{III} complex with a phosphane oxide type bidentate ligand, 1,1′-biphenyl-2,2′-diylbis(diphenylphosphane oxide): BIPHEPO [$Eu(hfa)_3$(BIPHEPO)], for which the chemical structure is shown in Figure 1 (b).[15] The coordination geometry of $Eu(hfa)_3$(BIPHEPO) is also an 8-SAP with a certain distortion, and the introduction of bidentate phosphane oxide ligand in Eu^{III} complex leads to reduction of the geometrical symmetry and enhancement of the probability of the electric dipole transition. In order to suppress the symmetry of the ligand field and vibronic quenching, considerable recent attention has been focused on lanthanide complexes with polydentate (tridentate, tetradentate, pentadentate and hexadetate) ligands and their characteristic luminescence properties.[16] In most of these previous works, however, the lanthanide complexes with polydentate ligands have C–H units close to the metal center. We here attempted to prepare luminescent Eu^{III} complexes with a tridentate phosphane oxide and three hfa as LVF ligands, which are anticipated to construct an asymmetrical nine-coordinate structure (Mono-capped Square Anti-Prism: 9-SAP). We have recently reported that the radiative rate constant of Sm^{III} complex with 9-SAP structure is larger than those of symmetrical ten-coordinated Sm^{III} complexes.[17] Polydentate ligands may also provide stable coordination bindings which show promise toward improved emission properties.

In the present study, we report on luminescent properties of lanthanide complexes with three kinds of novel tridentate phosphane oxide ligands: {bis[*o*-(diphenylphosphoryl)-phenyl]phenylphosphane oxide}tris(hexafluoroacetylacetonato)europium(III) [$Eu(hfa)_3$(DPPPO)], {bis[*o*-(diphenylphosphoryl)pyridyl]phenylphosphane oxide}tris(hexafluoroacetylacetonato)europium(III) [$Eu(hfa)_3$(DPPYPO)] and {bis[*o*-(diphenylphosphoryl)benzothienyl]phenylphosphane oxide}tris(hexafluoroacetylacetonato)europium(III) [$Eu(hfa)_3$(DPBTPO); see part c of Figure 1]. The geometrical structures of the Eu^{III} complexes were characterized using NMR and X-ray single crystal analyses. We also compared the emission spectral shapes, the emission quantum yields, the emission lifetimes, the radiative and the non-radiative rate constants in nine-coordinate Eu^{III} complexes with those of eight-coordinate Eu^{III} complexes [$Eu(hfa)_3$(BIPHEPO), $Eu(hfa)_3(TPPO)_2$]. The photophysical properties of nine-coordinate Eu^{III} complexes with tridentate phosphane oxide ligand are elucidated in terms of geometrical, vibrational and chemical structures.

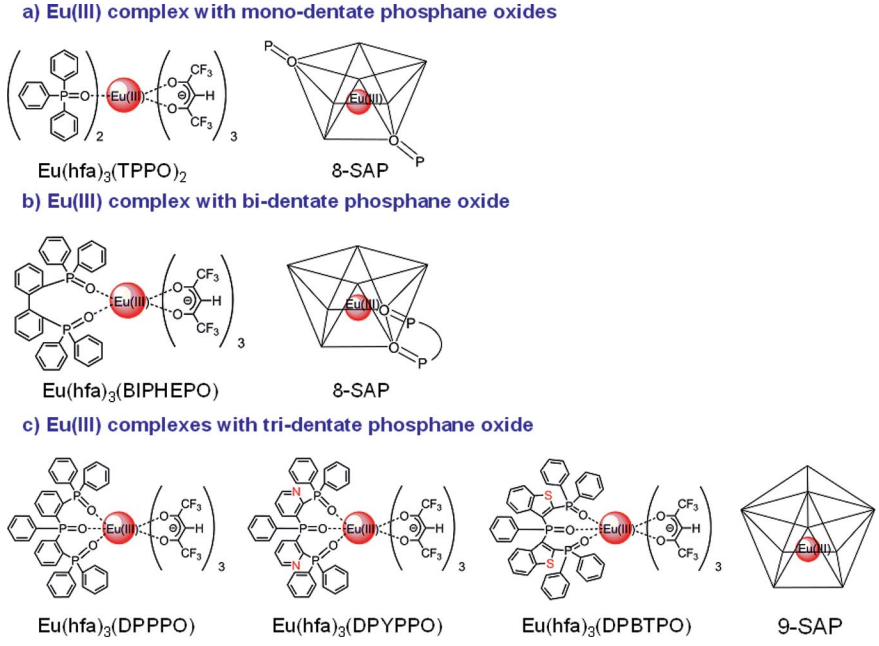

Figure 1. Chemical and coordination structures of Eu^{III} complexes with mono-, di-, and tridentate phosphane oxides.

Results and Discussion

Syntheses and Coordination Structures of Eu^{III} Complexes with Tridentate Phosphane Oxides

Eu^{III} complexes with tridentate phosphane oxides, $Eu(hfa)_3(DPPPO)$, $Eu(hfa)_3(DPPYPO)$ and $Eu(hfa)_3$-(DPBTPO) were synthesized by complexation of phosphane oxide ligands with $Eu(hfa)_3(H_2O)_2$ in methanol for 8 h as illustrated in Figure 2.[14a] The IR spectra and elemental analyses indicate that no water molecule exists in the coordination sphere of Eu^{III} complexes. We also observed the signals of corresponding $[Eu(hfa)_2(DPPPO)]^+$, $[Eu(hfa)_2(DPPYPO)]^+$ and $[Eu(hfa)_2(DPBTPO)]^+$ in ESI-mass spectra. The ^{31}P NMR spectra of the Eu^{III} complexes in $[D_6]$acetone exhibited three specific signals. These results indicate that the magnetic environments of phosphane oxides are different from each other in the solution phase.

Single crystals of $Eu(hfa)_3(DPPPO)$ and $Eu(hfa)_3$-(DPBTPO) were successfully prepared for X-ray single-crystal puposes by recrystallization from acetone solutions. The ORTEP views and crystal data from the X-ray single-crystal analyses are summarized in Figure 3 and Tables 1 and 2. The ORTEP views of both $Eu(hfa)_3(DPPPO)$ and $Eu(hfa)_3(DPBTPO)$ show the nine-coordinate structures with one tridentate phosphane oxide (DPPPO or DPBTPO) and three hfa ligands. The coordination geometries of $Eu(hfa)_3(DPPPO)$ and $Eu(hfa)_3(DPBTPO)$ are categorized

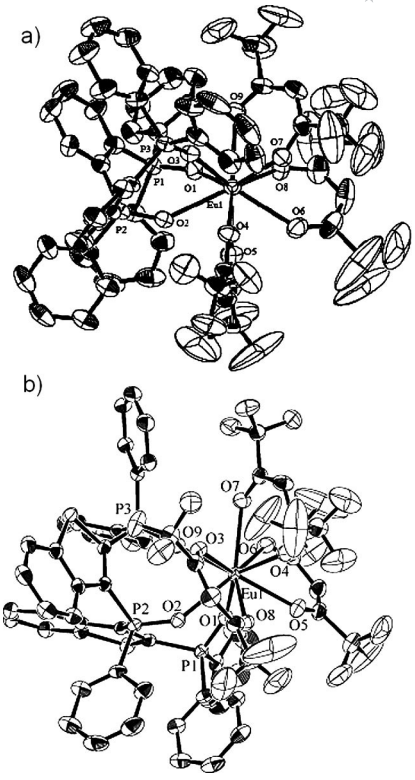

Figure 3. ORTEP view of single crystals of a) $Eu(hfa)_3(DPPPO)$ from acetone/water solution, and of b) $Eu(hfa)_3(DPBTPO)$ from acetone solution.

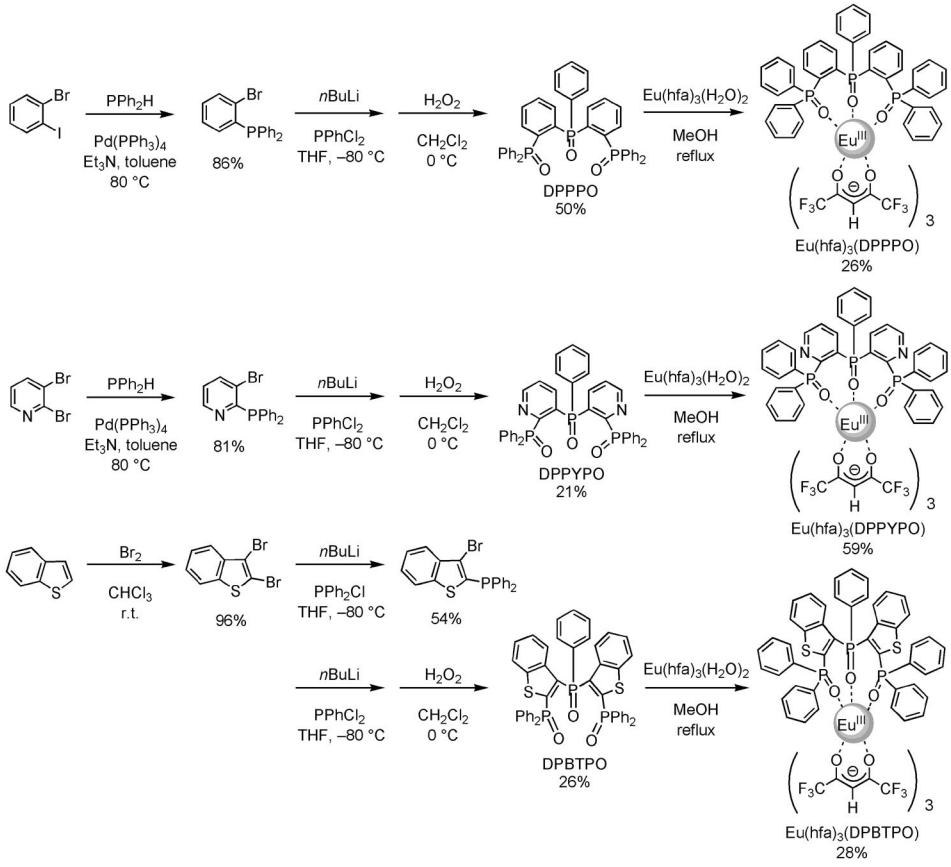

Figure 2. Synthetic schemes of $Eu(hfa)_3(DPPPO)$, $Eu(hfa)_3(DPPYPO)$ and $Eu(hfa)_3(DPBTPO)$.

Table 1. Crystal data of Eu^{III} complexes with tridentate phosphane oxide ligands.

	$Eu(hfa)_3(DPPPO)$	$2Eu(hfa)_3(DPBTPO)\cdot 0.5$ acetone
Chemical formula	$C_{57}H_{36}EuF_{18}O_9P_3$	$C_{125}H_{78}Eu_2F_{36}O_{19}P_6S_4$
Formula weight	1451.76	3185.93
Crystal color, habit	colorless, block	colorless, block
Crystal system	trigonal	monoclinic
Space group	*R*3*c*	*C*2/*c*
a [Å]	40.3572(7)	24.6695(14)
b [Å]		12.3999(6)
c [Å]	24.5364(5)	42.565(2)
β [°]		99.3595(14)
V [Å^3]	34608.5(10)	12847.4(11)
Z	18	4
T [°C]	–80 ± 1	–120 ± 1
μ (Mo-$K_α$) [cm^{-1}]	9.617	12.226
Number of measured reflections	91569	44801
Number of unique reflections	13372	10505
R [$I > 2σ(I)$][a]	0.0344	0.0351
R_w [$I > 2σ(I)$][b]	0.1106	0.0870

[a] $R = \Sigma||F_o| - |F_c||/\Sigma |F_o|$. [b] $R_w = [(\Sigma w(|F_o| - |F_c|)^2/\Sigma w F_o^2)]^{1/2}$.

as mono-capped square antiprisms (9-SAP).[18] In $Eu(hfa)_3$(DPPPO) and $Eu(hfa)_3$(DPBTPO), the Eu–O bond lengths that are attached with two terminal phosphane oxides in Table 2 are similar to those of the reported $Eu(hfa)_3$(BIPHEPO), 2.32 and 2.34 Å.[15] The Eu–O bond length for the central phosphane oxide in $Eu(hfa)_3$(DPPPO) (Eu–O2: 2.51 Å) and $Eu(hfa)_3$(DPBTPO) (Eu–O1: 2.48 Å) are considerably longer than those of the terminal phosphane oxides. The coordination structures of $Eu(hfa)_3$(DPPPO) and $Eu(hfa)_3$(DPBTPO) are thus considerably distorted compared with the usual 9-SAP shapes and would be categorized according to their quasi-C_1 symmetry, consistent with eight-coordinate $Eu(hfa)_3$(BIPHEPO) (Figure 4, a, b, c). Two terminal phosphane oxides of $Eu(hfa)_3$(DPPPO) are located on the upper square of 9-SAP, while those of

Table 2. Selected bond lengths [Å] of Eu^{III} complexes.

Bond	$Eu(hfa)_3$(DPPPO)	$Eu(hfa)_3$(DPBTPO)
Eu–O1 (P=O)	2.360 (terminal)	2.482 (central)
Eu–O2 (P=O)	2.511 (central)	2.403 (terminal)
Eu–O3 (P=O)	2.322 (terminal)	2.355 (terminal)

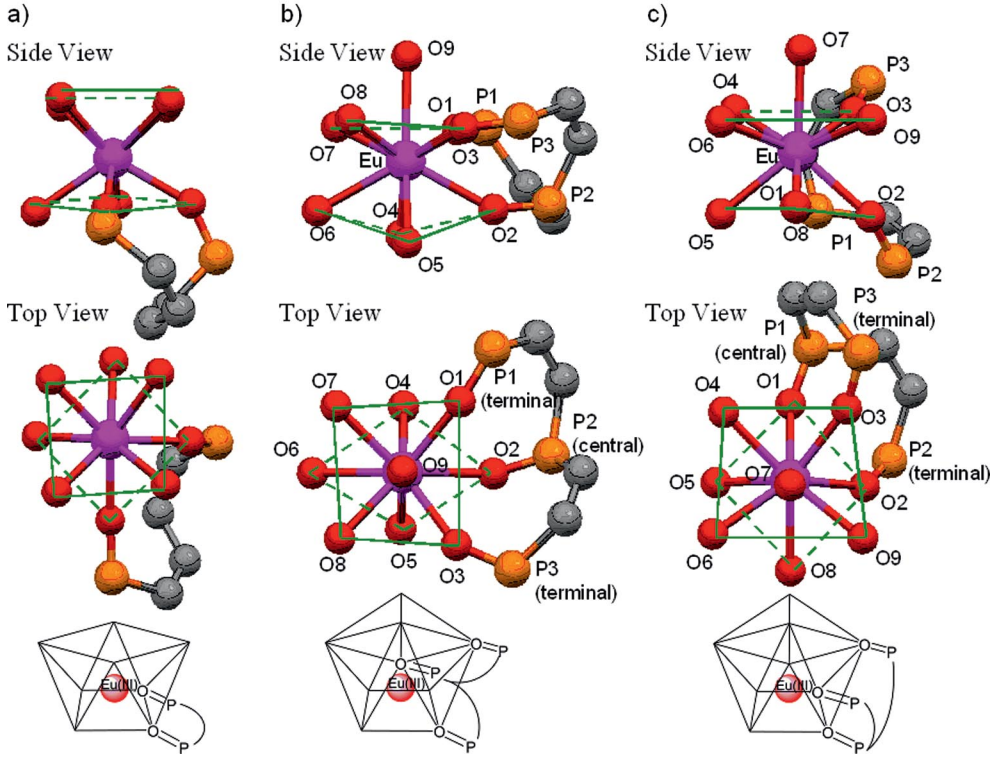

Figure 4. Coordination polyhedrons of a) $Eu(hfa)_3$(BIPHEPO), b) $Eu(hfa)_3$(DPPPO) and c) $Eu(hfa)_3$(DPBTPO).

$Eu(hfa)_3$(DPBTPO) are attached to the upper and lower squares of 9-SAP. We thus consider that the coordination structures of Eu^{III} complexes with tridentate phosphane oxide ligands are markedly influenced by the moiety between the phosphane oxides.

Based on the X-ray single crystal analyses, we carried out calculations of charge densities of phosphorus atoms by using DFT calculation [6-31G(d)/B3LYP]. According to the calculation, charge densities of phosphorus atoms were found to be P1: 0.22, P2: 0.14, P3 0.29 (DPPPO), P1: 0.04, P2: 0.35, P3: 0.11 (DPBTPO), respectively (see Figure S1, Supporting Information). We thus consider that three peaks in ^{31}P NMR spectra of Eu^{III} complexes might be caused by different electron densities of phosphorus atoms.

Photophysical Properties of Nine-Coordinated Eu^{III} Complexes

The steady-state emission spectra of $Eu(hfa)_3$(DPPPO), $Eu(hfa)_3$(DPPYPO) and $Eu(hfa)_3$(DPBTPO) in [D_6]acetone are shown in Figure 5 (a). Emission bands were observed at around 578, 592, 614, 650, and 700 nm, and are attributed to the *f*-*f* transitions of $^5D_0$–^7F_J with J = 0, 1, 2, 3 and 4, respectively. The spectra were normalized with respect to the magnetic dipole transition intensity ($^5D_0$–$^7F_1$) at 592 nm which is known to be insensitive to the surrounding environment of the Eu^{III} ion.[14a] The emission band at 614 nm ($^5D_0$–$^7F_2$) is due to the electric dipole transition for which intensity is greatly dependent on the chemical structures. In order to analyze the transition intensity, we here estimated the relative emission intensity of $^5D_0$–$^7F_2$ transition with respect to that of $^5D_0$–$^7F_1$ as $I_{rel} = I_{614}/I_{592}$ in the normalized emission spectra. The I_{rel} values of $Eu(hfa)_3$(DPBTPO), $Eu(hfa)_3$(DPPYPO) and $Eu(hfa)_3$(DPPPO) were found to be 18, 16 and 13, respectively, as summarized in Table 3. The emission spectra with Stark splittings at the electric dipole transition ($^5D_0$–$^7F_2$) of Eu^{III} complexes in [D_6]acetone are also shown in Figure 5 (b). Five-fold degenerated $^7F_2$ states of Eu^{III} complexes are known to split into some Stark levels between one to five depending on symmetry of the coordination structure.[16] We found that the emission spectral profiles and the wavenumbers of transition bands I and II of $Eu(hfa)_3$(DPPPO) and $Eu(hfa)_3$(DPBTPO) well agreed with those of $Eu(hfa)_3$(DPPYPO) (16280 cm^{-1}, 16370 cm^{-1}). The energy gaps between the transition bands I and II of these Eu^{III} complexes were approximately 85 cm^{-1}. Since the energy gap between the Stark splitting levels reflects its geometrical symmetry,[17] $Eu(hfa)_3$(DPPYPO) might be similar to $Eu(hfa)_3$(DPPPO) and $Eu(hfa)_3$(DPBTPO) in its structure in acetone. The emission quantum yields of $Eu(hfa)_3$(DPPPO), $Eu(hfa)_3$(DPPYPO) and $Eu(hfa)_3$(DPBTPO) in [D_6]acetone were found to be 0.60, 0.61 and 0.62, respectively (Table 3). These emission quantum yields are similar to those reported for $Eu(hfa)_3$(BIPHEPO) (Φ = 0.60 in [D_6]acetone) and $Eu(hfa)_3(TPPO)_2$ (Φ = 0.65 in [D_6]acetone), both of which have been reported as highly luminescent Eu^{III} complexes.[15]

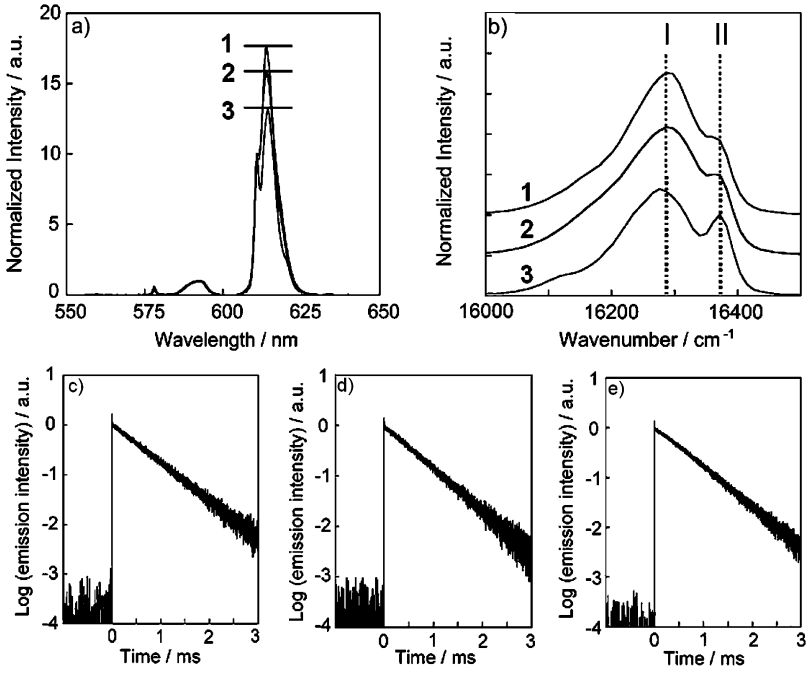

Figure 5. a) Emission spectra of $Eu(hfa)_3$(DPBTPO) (line 1), $Eu(hfa)_3$(DPPYPO) (line 2) and $Eu(hfa)_3$(DPPPO) (line 3) in [D_6]acetone at room temperature. Excited at 465 nm. The spectra were normalized with respect to the magnetic dipole transition ($^5D_0$–$^7F_1$). b) Stark splitting at the electric dipole transition ($^5D_0$–$^7F_2$) of the Eu^{III} complexes. c) The decay profiles of $Eu(hfa)_3$(DPPPO), d) $Eu(hfa)_3$(DPPYPO) and e) $Eu(hfa)_3$(DPBTPO) in [D_6]acetone.

Table 3. Photophysical properties of the Eu^{III} complexes at room temperature.[a]

Complex	Φ[b]/%	τ_{obs}[c] [ms]	k_r [s^{-1}]	k_{nr} [s^{-1}]	I_{rel}[d]
$Eu(hfa)_3$(DPBTPO)	62	1.3	5.0×10^2	3.0×10^2	18
$Eu(hfa)_3$(DPPYPO)	61	1.2	5.1×10^2	3.2×10^2	16
$Eu(hfa)_3$(DPPPO)	60	1.2	5.0×10^2	3.3×10^2	13
$Eu(hfa)_3$(BIPHEPO)[e]	60	1.3	4.6×10^2	3.4×10^2	–
$Eu(hfa)_3(TPPO)_2$[e]	65	1.2	5.4×10^2	3.0×10^2	–

[a] The emission spectra, quantum yield (Φ) and lifetime (τ_{obs}) were measured by excitation at 465 nm. Radiative rate $k_r = \Phi/\tau_{obs}$. Non-radiative rate $k_{nr} = 1/\tau_{obs} - k_r$. [b] Emission quantum yields were determined by comparing with the emission signal integration (570–640 nm) of $Eu(hfa)_3$(BIPHEPO) as $\Phi = 0.60$. [c] Emission lifetime (τ_{obs}) of the Eu^{III} complexes were measured by excitation at 355 nm (Nd:YAG 3ω). [d] Relative emission intensity of the electric dipole transition ($^5D_0$–$^7F_2$) to the magnetic dipole transition ($^5D_0$–$^7F_1$). [e] Ref.[25]

The time-resolved emission profiles of all Eu^{III} complexes reveal single-exponential decays with lifetimes on the millisecond time scale as shown in Figure 5 (c, d and e). The emission lifetimes were determined from the slopes of logarithmic plots of the decay profiles. The radiative (k_r) and non-radiative (k_{nr}) rate constants estimated using the emission lifetimes and the emission quantum yields are summarized in Table 3. We observed that the radiative rate constants of nine-coordinate $Eu(hfa)_3$(DPPPO) ($5.0\times10^2\ s^{-1}$), $Eu(hfa)_3$(DPPYPO) ($5.1\times10^2\ s^{-1}$) and $Eu(hfa)_3$(DPBTPO) ($5.0\times10^2\ s^{-1}$) were similar to those of the eight-coordinate $Eu(hfa)_3$(BIPHEPO) ($4.6\times10^2\ s^{-1}$) and $Eu(hfa)_3(TPPO)_2$ ($5.4\times10^2\ s^{-1}$). Generally, reduction of the geometrical symmetry of coordination structure leads to a larger radiative rate constant.[15] The radiative rate constant of Eu^{III} complex with phosphane oxides seems to depend on the symmetry of the coordination sites, but not on the coordination number. The non-radiative rate constants of $Eu(hfa)_3$(DPPPO) ($3.3\times10^2\ s^{-1}$), $Eu(hfa)_3$(DPPYPO) ($3.2\times10^2\ s^{-1}$) and $Eu(hfa)_3$(DPBTPO) ($3.0\times10^2\ s^{-1}$) were also quite similar to that of $Eu(hfa)_3$(BIPHEPO) ($3.4\times10^2\ s^{-1}$) and $Eu(hfa)_3(TPPO)_2$ ($3.0\times10^2\ s^{-1}$). The non-radiative rate constant of Eu^{III} might not be affected by vibrational, electric and steric structures of the chemical species attached with LVF phosphane oxides.

In this study, we found that the emission intensities at the electric dipole transition of Eu^{III} complexes depended on the organic linker species in phosphane oxide ligands, although the energy gap between Stark splitting levels, radiative and non-radiative rate constants were not affected by them. It seems that the transition intensity at the electric dipole transition is affected by chemical structures of attached tridentate phosphane oxide ligands. Recently, we have observed that the transition intensity of photochromic Eu^{III} complex is influenced by the polarizability of attached photochromic ligands.[19] The effect of polarizability on lanthanide complexes has also been suggested.[9b,20] Blasse has also reported the influence of charge transfer state on the transition intensity of lanthanide complex.[21] We reason that the emission spectral shapes of Eu^{III} complexes with tridentate phosphane oxide ligands might be related not only to geometrical and vibrational structures of Eu^{III} complexes, but also to the chemical structures of their ligands.

Conclusions

We successfully synthesized novel Eu^{III} complexes containing characteristic tridentate phosphane oxide ligands, DPPPO, DPPYPO and DPBTPO with high emission quantum yields (>60%). These Eu^{III} complexes showed characteristic emission properties depending on their moiety between phosphane oxides. In the present study, we have reported on nine-coordinate lanthanide complexes with characteristic photophysical properties. The photophysical properties of Eu^{III} complexes with tridentate phosphane oxide ligands would be discussed on the basis of geometrical, vibrational and chemical structures of the ligands.

Experimental Section

Materials: [D_6]acetone (D, 99.9%) and [D]chloroform (D, 99.8%) were obtained from Cambridge Isotope laboratories, Inc. Dry THF was prepared by distillation over benzophenone and Na metal. All other chemicals and solvents were reagent grade and were used without further purification.

Apparatus: Infrared spectra were recorded on JASCO FT/IR-420 spectrometer. ^1H (300 MHz), ^{19}F (500 MHz) and ^{31}P NMR (500 MHz) spectra were recorded on JEOL ECP–500. Chemical shifts are reported in δ ppm, referenced to internal tetramethylsilane standard for ^1H NMR, external trifluoroacetic acid standard ($\delta = -76.5$) for ^{19}F NMR and internal 85% H_3PO_4 standard for ^{31}P NMR spectroscopy. ESI–mass spectra were measured on JEOL JMS–700M Station. Elemental analyses were performed by Perkin–Elmer 2400II.

Preparation of Bis[*o*-(diphenylphosphoryl)phenyl]phenylphosphane Oxide (DPPPO): Synthesis was performed according to the published procedure.[22] Organic reagents, (*o*-bromophenyl)diphenylphosphane (3.0 g, 9.6 mmol)[23] and dry ethyl ether (90 mL), were placed in a 200 mL, three necked flask equipped with a dropping funnel and a nitrogen balloon. The solution was cooled to –80 °C and then 1.6 M *n*-butyllithium hexane solution (6 mL, 9.64 mmol) was added dropwise via dropping funnel. After the mixture was stirred at –80 °C for 30 min, dichlorophenylphosphane (860 mg, 4.8 mmol) was added. The reaction mixture was warmed to room temperature and stirred at room temperature for 3 h. The reaction was quenched by addition of water (ca. 30 mL), and then the resulting white solid was collected by filtration. The solid was dissolved in chloroform (ca. 100 mL) and washed with water for three times. The organic layer was separated and dried with anhydrous magnesium sulfate, and concentrated to dryness. The obtained powder and dichloromethane (50 mL) were placed in a 100 mL flask. The solution was cooled to 0 °C and then 30% H_2O_2 aqueous solution (7.8 mL, 69 mmol) was added to it. The reaction mixture was stirred at 0 °C for 4 h. The organic layer was separated and washed with water for three times, then dried with anhydrous magnesium sulfate and concentrated to dryness. The obtained powder was dissolved in hot chloroform/hexane solution (50 °C, ca. 5 mL), and then the solution was permitted to stand at room temperature. Recrystallization from chloroform/hexane gave colorless crystals of the titled compound. Yield 1.4 g (50%). MALDI-TOF mass *m*/*z* =

679.2 $[M + H]^+$. ^1H NMR (500 MHz, $CDCl_3$, 25 °C): δ = 7.98 (m, 2 H, Ar), 7.25–7.60 (m, 31 H, Ar) ppm. ^{31}P NMR (200 MHz, $CDCl_3$, 25 °C): δ = 36.78 (1 P), 33.65 (2 P) ppm. $C_{42}H_{33}O_3P_3 \cdot 0.3CHCl_3$ (713.54): calcd. C 70.77, H 4.68; found C 70.88, H 4.60.

Preparation of Bis[*o*-(diphenylphosphoryl)phenyl]phenylphosphane Oxide Tris(hexafluoroacetylacetonato)europium(III) [Eu(hfa)$_3$-(DPPPO)]: DPPPO (160 mg, 0.24 mmol), $Eu(hfa)_3(H_2O)_2$[14a] (220 mg, 0.27 mmol) and methanol (10 mL) were placed in a 20 mL flask. The solution was refluxed whilst stirring for 8 h. The mixture was concentrated to dryness. The residue was washed with chloroform for several times. The insoluble material was removed by filtration, and the filtrate was concentrated. The obtained powder was dissolved in hot acetone/water solution (50 °C, ca. 1 mL), and then the solution was permitted to stand at room temperature. Recrystallization from acetone/water gave colorless crystals of the titled compound. Yield 90 mg (26%). IR (ATR): $\tilde{\nu}$ = 1657, 1537, 1439, 1252, 1176, 1136, 789, 746, 727, 692, 660 cm^{-1}. ^{19}F NMR (470 MHz, [D$_6$]acetone, 25 °C): δ = –79.36 ppm. ^{31}P NMR (200 MHz, [D$_6$]acetone, 25 °C): δ = 0.55 (1 P), –29.03 (1 P), –68.37 (1 P) ppm. ESI mass *m*/*z* = 1245.052 $[M – (hfa)]^+$. $C_{57}H_{36}EuF_{18}O_9P_3$ (1452.05): calcd. C 47.16, H 2.50; found C 47.10, H 2.50.

Preparation of (*o*-Bromopyridyl)diphenylphosphane: 2,3-Dibromopyridine (8.0 g, 34 mmol), diphenylphosphane (6.3 g, 34 mmol), triethylamine (6.9 g, 68 mmol), and a catalytic amount of $Pd(PPh_3)_4$ (390 mg, 0.34 mmol) were dissolved in 40 mL of toluene under nitrogen atmosphere. The solution was heated at 80 °C whilst stirring for 16 h. The reaction mixture was washed with brine and extracted with diethyl ether for three times. The organic layer was dried with anhydrous magnesium sulfate, and concentrated to dryness. The obtained powder was dissolved in hot ethyl acetate/hexane solution (50 °C, ca. 50 mL), and then the solution was permitted to stand at room temperature. Recrystallization from ethyl acetate/hexane gave colorless block crystals of the titled compound. Yield 9.3 g (81%). IR (ATR): $\tilde{\nu}$ = 1559, 1478, 1436, 1382, 1011 cm^{-1}. MALDI-TOF mass *m*/*z* = 342.0 $[M + H]^+$. ^1H NMR (300 MHz, $CDCl_3$, 25 °C): δ = 8.58–8.56 (m, 1 H, Ar), 7.78–7.83 (m, 1 H, Ar), 7.35–7.40 (m, 10 H, Ar), 7.06–7.10 (m, 1 H, Ar) ppm. ^{13}C NMR (75 MHz, $CDCl_3$, 25 °C): δ = 148.66, 139.54, 135.43, 134.36, 129.01, 128.56, 128.36, 128.04, 123.67 ppm. $C_{17}H_{13}BrNP$ (341.00): calcd. C 59.67, H 3.83, N 4.09; found C 59.82, H 3.71, N 4.10.

Preparation of Bis[*o*-(diphenylphosphoryl)pyridyl]phenylphosphane Oxide (DPPYPO): (*o*-Bromopyridyl)diphenylphosphane (1.7 g, 5.0 mmol) and dry THF (40 mL) were placed in a 200 mL, three necked flask equipped with a dropping funnel and a nitrogen balloon. The solution was cooled to –80 °C and then 1.6 M *n*-butyllithium hexane solution (3.3 mL, 5.3 mmol) was added dropwise via syringe. After the mixture was stirred at –80 °C for 1 h, dichlorophenylphosphane (450 mg, 2.5 mmol) was added dropwise via dropping funnel. The reaction mixture was warmed to room temperature and stirred at room temperature for 3 h. The reaction was quenched by addition of water (ca. 5 mL) and extracted with chloroform for three times. The organic layer was dried with anhydrous magnesium sulfate, and concentrated to dryness. The obtained powder was dissolved in dichloromethane (15 mL) in a 100 mL flask. The solution was cooled to 0 °C, and then 30% H_2O_2 aqueous solution (2.7 mL, 24 mmol) was added. The reaction mixture was stirred at 0 °C for 4 h, and then reaction mixture was extracted with dichloromethane for three times. The organic layer was dried with anhydrous magnesium sulfate, and concentrated to dryness. The obtained powder was dissolved in hot acetone/hexane solution (50 °C, ca. 5 mL), and then the solution was permitted to stand at room temperature. Recrystallization from acetone/hexane gave white crystals of the titled compound. Yield 0.36 g (21%). IR (ATR): $\tilde{\nu}$ = 1548, 1434, 1390, 1197, 1119, 1107 cm^{-1}. MALDI-TOF mass *m*/*z* = 681.5 $[M + H]^+$. ^1H NMR (300 MHz, $CDCl_3$, 25 °C): δ = 8.73 (s, 2 H, Ar), 7.92–7.99 (m, 2 H, Ar), 7.21–7.64 (m, 27 H, Ar) ppm. ^{31}P NMR (200 MHz, $CDCl_3$, 25 °C): δ = 29.71 (s,1 P), 25.20 (br. 2 P) ppm. $C_{40}H_{31}N_2O_3P_3 \cdot H_2O$ (698.17): calcd. C 68.77, H 4.76, N 4.01; found C 69.02, H 4.66, N 3.97.

Preparation of Eu(hfa)$_3$(DPPYPO): DPPYPO (300 mg, 0.44 mmol) and $Eu(hfa)_3(H_2O)_2$ (430 mg, 0.53 mmol) were dissolved in methanol (25 mL). The solution was refluxed whilst stirring for 8 h. The mixture was concentrated to dryness. The residue was washed with chloroform for several times. The insoluble material was removed by filtration, and the filtrate was concentrated. The obtained powder was dissolved in hot chloroform/hexane solution (50 °C, ca. 2 mL), and then the solution was permitted to stand at room temperature. Recrystallization from chloroform/hexane gave white crystals of the titled compound. Yield 0.38 g (59%). IR (ATR): $\tilde{\nu}$ = 1653, 1550, 1525, 1507, 1440, 1252, 1191, 1138, 1124, 1097 cm^{-1}. ^{19}F NMR (470 MHz, [D$_6$]acetone, 25 °C): δ = –78.71 (s) ppm. ^{31}P NMR (200 MHz [D$_6$]acetone, 25 °C): δ = –12.08 (s, 1 P), –15.81 (s, 1 P), –64.75 (s, 1 P) ppm. ESI mass *m*/*z* = 1247.052 $[M – (hfa)]^+$. $C_{55}H_{34}EuF_{18}N_2O_9P_3 \cdot 1.5CHCl_3$ (1630.91): calcd. C 41.59, H 2.13, N 1.72; found C 41.71, H 2.13, N 1.70.

Preparation of 2,3-Dibromobenzothiophene: 2,3-dibromobenzothiophene was synthesized according to the published procedure.[24] Benzothiophene (19 g, 140 mmol) were dissolved in chloroform (200 mL). Then, Br_2 (16 mL, 310 mmol) was added dropwise to the solution. The reaction mixture was stirred at room temperature for 24 h. The resulting solution was washed with $Na_2S_2O_3$ aqueous solution, and extracted with ethyl acetate for three times. The organic layer was dried with anhydrous magnesium sulfate, and concentrated to dryness. Reprecipitation from excess amount of hexane (ca. 100 mL) gave a white powder of the titled compound. Yield 40 g (96%). IR (ATR): $\tilde{\nu}$ = 1419, 1298, 1245, 987, 893, 743, 716 cm^{-1}. MALDI-TOF mass *m*/*z* = 290.8 $[M + H]^+$. ^1H NMR (300 MHz, $CDCl_3$, 25 °C): δ = 7.69–7.76 (m, 2 H, Ar), 7.35–7.45 (m, 2 H, Ar) ppm.

Preparation of (*o*-Bromobenzothienyl)diphenylphosphane: 2,3-Dibromobenzothiophene (20 g, 69 mmol) and dry THF (500 mL) were placed in a 1000 mL, three-necked flask equipped with a dropping funnel and a nitrogen balloon. The solution was cooled to –80 °C and then 1.6 M *n*-butyllithium hexane solution (43 mL, 69 mmol) was added dropwise via dropping funnel. After the mixture was stirred at –80 °C for 1 h, chlorodiphenylphosphane (15 g, 69 mmol) was added dropwise. The reaction mixture was warmed to room temperature and stirred at room temperature for 12 h. The reaction was quenched by addition of water, and extracted with diethyl ether for three times. The organic layer was dried with anhydrous magnesium sulfate, and concentrated to dryness. The obtained powder was dissolved in hot chloroform/hexane solution (50 °C, ca. 50 mL), and then the solution was permitted to stand at room temperature. Recrystallization from chloroform/hexane gave white yellow crystals of the titled compound. Yield 15 g (54%). IR (ATR): $\tilde{\nu}$ = 1431, 1243, 999, 891, 743, 726, 692 cm^{-1}. MALDI-TOF mass *m*/*z* = 397.3 $[M + H]^+$. ^1H NMR (300 MHz, $CDCl_3$, 25 °C): δ = 7.83–7.86 (d, *J* = 9 Hz, 1 H, Ar), 7.68–7.71 (d, *J* = 9 Hz, 1 H, Ar), 7.37–7.47 (m, 12 H, Ar) ppm. ^{13}C NMR (75 MHz, $CDCl_3$, 25 °C): δ = 141.14, 139.29, 135.94, 135.22, 133.57, 129.45, 128.64, 125.64, 125.07, 123.20, 122.23, 116.55 ppm. $C_{20}H_{14}BrPS$ (395.97): calcd. C 60.47, H 3.55; found C 60.26, H 3.36.

Preparation of Bis[*o*-(diphenylphosphoryl)benzothienyl]phenylphosphane Oxide (DPBTPO): (*o*-bromobenzothienyl)diphenylphos-

phane (4.0 g, 10 mmol) and dry THF (100 mL) were placed in a 300 mL, three necked flask equipped with a dropping funnel and a nitrogen balloon. The solution was cooled to –80 °C and then 1.6 M *n*-butyllithium hexane solution (6.6 mL, 11 mmol) was added dropwise via syringe. After the mixture was stirred at –80 °C for 1 h, dichlorophenylphosphane (900 mg, 5.0 mmol) was added dropwise via dropping funnel. The reaction mixture was warmed to room temperature and stirred at room temperature for 3 h. The reaction was quenched by addition of water (ca. 5 mL), and extracted with chloroform for three times. The organic layer was dried with anhydrous magnesium sulfate, and concentrated to dryness. The obtained powder was dissolved in dichloromethane (30 mL) in a 100 mL flask. The solution was cooled to 0 °C, and then 30% H_2O_2 aqueous solution (5.5 mL, 49 mmol) was added. The reaction mixture was stirred at 0 °C for 4 h, and then reaction mixture was extracted with dichloromethane for three times. The organic layer was dried with anhydrous magnesium sulfate, and concentrated to dryness. The obtained powder was dissolved in hot acetone/hexane solution (50 °C, ca. 5 mL), and then the solution was permitted to stand at room temperature. Recrystallization from acetone/hexane gave white crystals of the titled compound. Yield 1.0 g (26%). IR (ATR): $\tilde{\nu}$ = 1457, 1437, 1388, 1203, 1116, 1102, 1010, 898, 801 cm^{-1}. MALDI-TOF mass *m*/*z* = 791.5 $[M + H]^+$. ^1H NMR (300 MHz, $CDCl_3$, 25 °C): δ = 8.34–8.42 (d, *J* = 24 Hz, 2 H, Ar), 7.64–7.71 (m, 6 H, Ar), 7.45–7.47 (m, 9 H, Ar), 7.24–7.30 (m, 14 H, Ar), 6.86 (br., 2 H, Ar) ppm. ^{31}P NMR (200 MHz, $CDCl_3$, 25 °C): δ = 21.80–21.83 (d, *J* = 6 Hz, 2 P), 14.81–14.87 (t, *J* = 6 Hz, 1 P) ppm. $C_{46}H_{33}O_3P_3S_2 \cdot 0.5CH_2Cl_2$ (832.09): calcd. C 67.02, H 4.11; found C 67.33, H 4.11 (the CH_2Cl_2 molecule comes from the reaction solvent).

Preparation of Eu(hfa)$_3$(DPBTPO): DPBTPO (300 mg, 0.38 mmol) and $Eu(hfa)_3(H_2O)_2$ (370 mg, 0.46 mmol) were dissolved in methanol (30 mL). The solution was refluxed whilst stirring for 8 h. The mixture was concentrated to dryness. The residue was washed with chloroform for several times. The insoluble material was removed by filtration, and the filtrate was concentrated. The obtained powder was dissolved in hot acetone solution (50 °C, ca. 2 mL), and then the solution was permitted to stand at room temperature. Recrystallization from acetone gave colorless crystals of the titled compound. Yield 0.17 g (28%). IR (ATR): $\tilde{\nu}$ = 1657, 1534, 1440, 1251, 1185, 1138, 1125, 1104 cm^{-1}. ^{19}F NMR (470 MHz, $[D_6]$acetone, 25 °C): δ = –78.55 (s) ppm. ^{31}P NMR (200 MHz, $[D_6]$acetone, 25 °C): δ = –47.78 (s, 1P), –53.29 (s, 1P), –78.18 (s, 1P) ppm. ESI mass *m*/*z* = 1357.001 $[M – (hfa)]^+$. $C_{61}H_{36}EuF_{18}O_9P_3S_2$ (1564.00): calcd. C 46.85, H 2.32; found C 46.68, H 2.24.

Crystallography: Colorless single crystals of Eu(hfa)$_3$(DPPPO) and Eu(hfa)$_3$(DPBTPO) obtained from acetone solution were mounted on a glass fiber using epoxy resin glue. All measurements were made on a Rigaku RAXIS RAPID imaging plate area detector with graphite-monochromated Mo-K_α radiation. The data were collected at a temperature range of –120 ± 1 °C to a maximum 2θ value of 48.8°. Corrections for decay and Lorentz-polarization effects were made with empirical absorption correction, solved by direct methods and expanded using Fourier techniques. The non-hydrogen atoms were refined anisotropically. Hydrogen atoms were refined using the riding model. The final cycle of full-matrix least-squares refinement was based on observed reflections and variable parameters. All calculations were performed using the crystal structure crystallographic software package.

CCDC-737332 [for Eu(hfa)$_3$(DPPPO)] and -737333 [for Eu(hfa)$_3$(DPBTPO)] contain the supplementary crystallographic data for this paper. CIF data confirmed by using checkCIF/PLATON service. These data can be obtained free of charge from The Cambridge Crystallographic Data Center via www.ccdc.cam.ac.uk/data_request/cif.

Optical Masurements: UV/Vis absorption spectra were recorded on a JASCO V-550 spectrometer. Emission spectra of the europium(III) complexes were measured with a Hitachi F-4500 spectrometer and corrected for the response of the detector system. The emission quantum yields of Eu(hfa)$_3$(DPPPO), Eu(hfa)$_3$(DPPYPO) and Eu(hfa)$_3$(DPBTPO) (5.0 mM in $[D_6]$acetone) were obtained by comparison with the emission signal integration (570–640 nm) of Eu(hfa)$_3$(BIPHEPO) as a reference (Φ = 0.60: 50 mM in $[D_6]$acetone) with excitation wavelength of 465 nm.[25] Emission lifetimes of Eu(hfa)$_3$(DPPPO), Eu(hfa)$_3$(DPPYPO) and Eu(hfa)$_3$(DPBTPO) (1.0 mM in $[D_6]$acetone) were measured with the third harmonics (355 nm) of a Q-swiched Nd:YAG laser (Spectra Physics, INDI-50, fwhm = 5 ns, λ = 1064 nm) and a photomultiplier (Hamamatsu photonics, R5108, response time ≤ 1.1 ns). The Nd:YAG laser response was monitored with a digital oscilloscope (Sony Tektronix, TDS3052, 500 MHz) synchronized to the single-pulse excitation. Emission lifetimes were determined from the slope of logarithmic plots of decay profiles. High-resolution spectra of the emission were measured with SPEX fluorolog.

Supporting Information (see also the footnote on the first page of this article): Figure S1, charge densities of phosphorus atoms in a) DPPPO and b) DPBTPO ligand.

Acknowledgments

We thank Mr. S. Katao, Mr. F. Asanoma, Mrs. Y. Nishikawa, and Mrs. M. Yamamura, technical staff of NAIST for X-ray crystallographic analyses, elemental analyses, NMR and mass spectroscopic measurements. This work was supported partly by a Grant-in-Aid for Scientific Research on Priority Area of "Strong Photo-Molecule Coupling Fields for Chemical Reactions" from the Ministry of Education, Culture, Sports, Science and Technology (MEXT), Japan.

[1] a) T. Jüstel, H. Nikol, C. Ronda, *Angew. Chem. Int. Ed.* **1998**, *37*, 3084–3103; b) J. Kido, Y. Okamoto, *Chem. Rev.* **2002**, *102*, 2357–2368.

[2] a) K. Kuriki, Y. Koike, Y. Okamoto, *Chem. Rev.* **2002**, *102*, 2347–2356; b) Y. Hasegawa, Y. Wada, S. Yanagida, *J. Photochem. Photobiol. C: Photochem. Rev.* **2004**, *5*, 183–202.

[3] a) F. S. Richardson, *Chem. Rev.* **1982**, *82*, 541–552; b) J. Yu, D. Parker, R. Pal, R. A. Poole, M. J. Cann, *J. Am. Chem. Soc.* **2006**, *128*, 2294–2299.

[4] F. Gan, *Laser Materials*, World Scientific, Singapore, **1995**, p. 70.

[5] a) J.-C. G. Bünzli, C. Piguet, *Chem. Rev.* **2002**, *102*, 1897–1928; b) V. S. Sastri, J.-C. G. Bünzli, V. R. Rao, G. V. S. Rayudu, J. R. Perumareddi, in: *Modern Aspects of Rare Earth and Their Complexes*, Elsevier, New York, **2003**.

[6] For recent papers on luminescent lanthanide(III) complexes, see: a) T. Gunnlaugsson, J. P. Leonard, K. Senechal, A. J. Harte, *J. Am. Chem. Soc.* **2003**, *125*, 12062–12063; b) S. Faulkner, S. J. A. Pope, *J. Am. Chem. Soc.* **2003**, *125*, 10526–10527; c) S. Petoud, S. M. Cohen, J.-C. G. Bünzli, K. N. Raymond, *J. Am. Chem. Soc.* **2003**, *125*, 13324–13325; d) J. B. Beck, S. J. Rowan, *J. Am. Chem. Soc.* **2003**, *125*, 13922–13923; e) A. P. Bassett, S. W. Magennis, P. B. Glover, D. J. Lewis, N. Spencer, S. Parsons, R. M. Williams, L. De Cola, Z. Pikramenou, *J. Am. Chem. Soc.* **2004**, *126*, 9413–9424; f) N. Weibel, L. J. Charbonniere, M. Guardigli, A. Roda, R. Ziessel, *J. Am. Chem. Soc.* **2004**, *126*, 4888–4896; g) C. Yang, L. M. Fu, Y. Wang, J. P.

Zhang, W. T. Wong, X. C. Ai, Y. F. Qiao, B. S. Zou, L. L. Gui, *Angew. Chem. Int. Ed.* **2004**, *43*, 5010–5013; h) P. Atkinson, Y. Bretonniere, D. Parker, *Chem. Commun.* **2004**, 438–439; i) P. Coppo, M. Duati, V. N. Kozhevnikov, J. W. Hofstraat, L. De Cola, *Angew. Chem. Int. Ed.* **2005**, *44*, 1806–1810; j) S. Banerjee, L. Huebner, M. D. Romanelli, G. A. Kumar, R. E. Riman, T. J. Emge, J. G. Brennan, *J. Am. Chem. Soc.* **2005**, *127*, 15900–15906; k) L. J. Charbonniere, N. Hildebrandt, R. F. Ziessel, H. Löehmannsröben, *J. Am. Chem. Soc.* **2006**, *128*, 12800–12809; l) R. Pal, D. Parker, *Chem. Commun.* **2007**, 474–476; m) J. P. Leonard, P. Jensen, T. McCabe, J. E. O'Brien, R. D. Peacock, P. E. Kruger, T. Gunnlaugsson, *J. Am. Chem. Soc.* **2007**, *129*, 10986–10987; n) A. De Bettencourt-Dias, S. Viswanathan, A. Rollett, *J. Am. Chem. Soc.* **2007**, *129*, 15436–15437; o) X. Y. Chen, X. Yang, B. J. Holliday, *J. Am. Chem. Soc.* **2008**, *130*, 1546–1547; p) M. Romanelli, G. A. Kumar, T. J. Emge, R. E. Riman, J. G. Brennan, *Angew. Chem. Int. Ed.* **2008**, *47*, 6049–6051; q) S. Banerjee, G. A. Kumar, R. E. Riman, T. J. Emge, J. G. Brennan, *J. Am. Chem. Soc.* **2007**, *129*, 5926–5931.

[7] a) E. M. Stephens, M. F. Reid, F. S. Richardson, *Inorg. Chem.* **1984**, *23*, 4611–4618; b) M. T. Devlin, E. M. Stephens, M. F. Reid, F. S. Richardson, *Inorg. Chem.* **1987**, *26*, 1208–1211.

[8] K. Binnemans, R. Van Deun, C. Görller-Walrand, S. R. Collinson, F. Martin, D. W. Bruce, C. Wickleder, *Phys. Chem. Chem. Phys.* **2000**, *2*, 3753–3757.

[9] a) S. F. Mason, R. D. Peacock, B. Stewart, *Chem. Phys. Lett.* **1974**, *29*, 149–153; b) S. F. Mason, *J. Indian Chem. Soc.* **1986**, *63*, 73–79.

[10] a) A. F. Kirby, F. S. Richardson, *J. Phys. Chem.* **1983**, *87*, 2544–2556; b) M. Montalti, L. Prodi, N. Zaccheroni, L. Charbonnière, L. Douce, R. Ziessel, *J. Am. Chem. Soc.* **2001**, *123*, 12694–12695; c) K. Driesen, P. Lenaerts, K. Binnemans, C. Görller-Walrand, *Phys. Chem. Chem. Phys.* **2002**, *4*, 552–555; d) W. Liu, T. Jiao, Y. Li, Q. Liu, M. Tan, H. Wang, L. Wang, *J. Am. Chem. Soc.* **2004**, *126*, 2280–2281; e) J. P. Cross, M. Lauz, P. D. Badger, S. Petoud, *J. Am. Chem. Soc.* **2004**, *126*, 16278–16279; f) P. Nockemann, B. Thijs, N. Postelmans, K. V. Hecke, L. V. Meervelt, K. Binnemans, *J. Am. Chem. Soc.* **2006**, *128*, 13658–13659; g) A. Wada, M. Watanabe, Y. Yamanoi, T. Nankawa, K. Namiki, M. Yamasaki, M. Murata, H. Nishihara, *Bull. Chem. Soc. Jpn.* **2007**, *80*, 335–345.

[11] G. Stain, E. Würzberg, *J. Chem. Phys.* **1975**, *62*, 208–214.

[12] a) Y. Hasegawa, M. Iwamuro, K. Murakoshi, Y. Wada, R. Arakawa, T. Yamanaka, N. Nakashima, S. Yanagida, *Bull. Chem. Soc. Jpn.* **1998**, *71*, 2573–2581; b) Y. Hasegawa, T. Ohkubo, K. Sogabe, Y. Kawamura, Y. Wada, N. Nakashima, S. Yanagida, *Angew. Chem. Int. Ed.* **2000**, *39*, 357–360; c) Y. Wada, T. Okubo, M. Ryo, T. Nakazawa, Y. Hasegawa, S. Yanagida, *J. Am. Chem. Soc.* **2000**, *122*, 8583–8584; d) Y. Hasegawa, Y. Kimura, K. Murakoshi, Y. Wada, J. Kim, N. Nakashima, T. Yamanaka, S. Yanagida, *J. Phys. Chem.* **1996**, *100*, 10201–10205; e) Y. Hasegawa, K. Murakoshi, Y. Wada, S. Yanagida, J. Kim, N. Nakashima, T. Yamanaka, *Chem. Phys. Lett.* **1996**, *248*, 8–12.

[13] K. Norton, G. A. Kumar, J. L. Dilks, T. J. Emge, R. E. Riman, M. G. Brik, J. G. Brennan, *Inorg. Chem.* **2009**, *48*, 3573–3580.

[14] a) Y. Hasegawa, M. Yamamuro, Y. Wada, N. Kanehisa, Y. Kai, S. Yanagida, *J. Phys. Chem. A* **2003**, *107*, 1697–1702; b) Y. Hasegawa, Y. Wada, S. Yanagida, H. Kawai, N. Yasuda, Y. Nagamura, *Appl. Phys. Lett.* **2003**, *83*, 3599–3602.

[15] K. Nakamura, Y. Hasegawa, H. Kawai, N. Yasuda, N. Kanehisa, Y. Kai, T. Nagamura, S. Yanagida, Y. Wada, *J. Phys. Chem. A* **2007**, *111*, 3029–3037.

[16] a) L. J. Charbonnire, R. Ziessel, M. Montalti, L. Prodi, C. Boehme, G. Wipff, *J. Am. Chem. Soc.* **2002**, *124*, 7779–7788; b) S. Faulkner, J. A. Pope, *J. Am. Chem. Soc.* **2003**, *125*, 10526–10527; c) G. S. Kottas, M. Mehlstäubl, R. Fröhlich, L. De Cola, *Eur. J. Inorg. Chem.* **2007**, *22*, 3465–3467; d) M. Seitz, E. G. Moore, A. J. Ingram, G. Muller, K. N. Raymond, *J. Am. Chem. Soc.* **2007**, *129*, 15468–15470; e) S. Petoud, G. Muller, E. G. Moore, J. Xu, J. Sokolnicki, J. P. Riehl, U. N. Le, S. M. Cohen, K. N. Raymond, *J. Am. Chem. Soc.* **2007**, *129*, 77–83; f) E. Deiters, B. Song, A. Chauvin, C. D. B. Vandevyver, F. Gumy, J.-C. G. Bünzli, *Chem. Eur. J.* **2009**, *15*, 885–900.

[17] Y. Hasegawa, S. Tsuruoka, T. Yoshida, H. Kawai, T. Kawai, *J. Phys. Chem. A* **2008**, *112*, 803–807.

[18] a) R. B. King, *J. Am. Chem. Soc.* **1969**, *91*, 7211–7216; b) R. B. King, *J. Am. Chem. Soc.* **1970**, *92*, 6455–6460.

[19] T. Nakagawa, Y. Hasegawa, T. Kawai, *J. Phys. Chem. A* **2008**, *112*, 5096–5103.

[20] J. J. Dallara, M. F. Reid, F. S. Richardson, *J. Phys. Chem.* **1984**, *88*, 3587–3594.

[21] C. D. Donega, S. J. L. Ribeiro, R. R. Goncalves, G. Blasse, *J. Phys. Chem. Solids* **1996**, *57*, 1727–1734.

[22] J. G. Hartley, L. M. Venanzi, D. C. Goodall, *J. Chem. Soc.* **1963**, 3930–3936.

[23] M. T. Whited, E. Rivard, J. C. Peters, *Chem. Commun.* **2006**, 1613–1615.

[24] A. Heynderickx, A. Samat, R. Guglielmetti, *Synthesis* **2002**, *2*, 213–216.

[25] K. Nakamura, Y. Hasegawa, H. Kawai, N. Yasuda, Y. Tsukahara, Y. Wada, *Thin Solid Films* **2008**, *516*, 2376–2381.

Received: June 29, 2009
Published Online: September 11, 2009

